Small Orbital Launcher - Risk Zone Evaluation

Teodor Viorel CHELARU[1], Adrian CHELARU*,[2], Alexandru Iulian ONEL[2]

*Corresponding author
[1]"POLITEHNICA" University of Bucharest, Faculty of Aerospace Engineering,
Polizu 1-7, 011611, Bucharest, Romania
teodor.chelaru@upb.ro
[2]INCAS − National Institute for Aerospace Research "Elie Carafoli",
Flow Physics Department,
B-dul Iuliu Maniu220, Bucharest 061126, Romania
chelaru.adrian@incas.ro*, onel.alexandru@incas.ro

DOI: 10.13111/2066-8201.2015.7.3.7

Received: 22 July 2015 / Accepted: 16 August 2015

Abstract: *The purpose of this paper is to present some aspects regarding two calculus models to evaluate the risk zone of the multistage launcher. Regarding the risk zone, unlike the classic model used for the launcher, we will use a calculus model build on non-inertial frames /taking part to the diurnal rotation (Earth spin). This is necessary to link the risk zone of the launch position, and place it on the map. For the risk zone we will use actually two models: first build in start frame which is more suitable for ascensional guidance phase, and second, built in quasi – velocity frame used for unguided motion especially in descending phase. The discussions will focus around the possibility to find a launching area to be satisfactory in terms of risk conditions arising from the SOL launching*

Key Words: *small orbital launcher, risk zone, danger zone, quasi-velocity frame*

1. INTRODUCTION

The first aspect regarding the flight experimentation of the launch vehicle (LV) Figure 1 is to determine the risk zone. The risk zone is defined in [2] as the zone where the vehicle can find itself because of the occurrence of certain incidents (malfunctions, wrong commands). In order to determine the risk zone one must assume some malfunctions that can lead to symmetrical commands generating a lateral movement; this is an extreme situation that allows the maximum development in the horizontal plane of the trajectories. The handling of the launch vehicle and the energy disposal on board the vehicle imposes its limits. The knowledge of the risk zone is necessary for avoiding certain accidents that can occur by the crashing of vehicle or parts of the vehicle (stages) over civilian areas or by injuring the personnel and destroying the involved in the experiment.

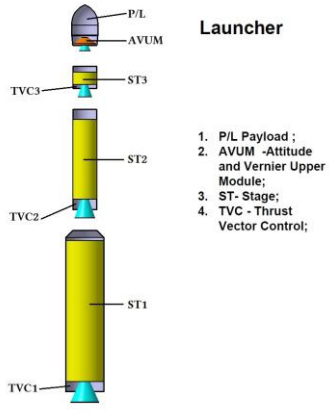

Figure 1. SOL - LV

The delimitation of the risk zone in order to execute the experiments in safety conditions can be done with a calculus model of the commanded flight, to which certain variations of control can be added in time, in order to obtain a maximum deployment of the trajectory in horizontal plane, corresponding to certain flight angles. Paper [2] exemplified the calculus models for the risk zone, the problem being solvable with the help of a flight model with 6 degrees of freedom.

Processing work [6], we obtained the motion dynamic equations in Start frame, by means of which we can in principle solve any technical problem. But often in order to investigate the motion it is appropriate to introduce simplifications for solving some specific problem.

For this reason, many studies of the launcher dynamics are straightforward if we use the description of the motion in a frame linked by the velocity vector. Next, beside well-known equations in Start frame, using work [6] we will write the equations set out above, in a frame related to the velocity, called quasi-velocity frame.

2. THE FRAMES

The Local Frame $O_L\ X_L\ Y_L\ Z_L$

This coordinate system has the origin in start position, being earthbound and participating in diurnal rotation (Earth spin) Figure 2. The axis Y_L is the position along the vector **r** at the start moment.

The axis Z_L is parallel to the equatorial plane, being oriented to the East. The deriving L_L axis forms with the first two axes a right trihedral.

The Start Frame - $O_L X_S Y_S Z_S$

This coordinate system has the origin in start position, being earthbound and participating in diurnal rotation (Earth spin).

The axis Y_L is the position along the vector **r** at the start moment. The axis X_S is oriented toward the launch direction and makes an azimuth angle ψ_0 related to X_L axis.

The deriving Z axis, forms with the first two axes a right trihedral, being oriented to the right relative to the launch plane.

The Initial Start Frame - $OX_0Y_0Z_0$

This coordinate system has the origin in start position, being loosed from Earth and does not participate in its diurnal rotation (Earth spin). This frame overlaps the start frame $OX_SY_SZ_S$ during the launch moment. It doesn't participate in Earth diurnal rotation being an inertial frame.

The Geographical Mobile Frame - $Ox_g y_g z_g$

This coordinate system has the origin in the center of the launcher mass of the launcher, being earthbound and participating in diurnal rotation (Figure 2).

The axis y_g is the position along the vector **r** . The axis z_g is parallel with the equatorial plane, being oriented to the East.

The deriving x_g axis, forms with the first two axes a right trihedral. The geographical mobile frame overlaps the local frame at the start moment.

The Geocentric Spherical Frame $O_p \lambda \varphi r$

This coordinate system originated in the center of the Earth, is earthbound and participates in its diurnal rotation (Earth spin). The launcher position can be described using spherical coordinates λ, φ, r, as can be seen in Figure 2.

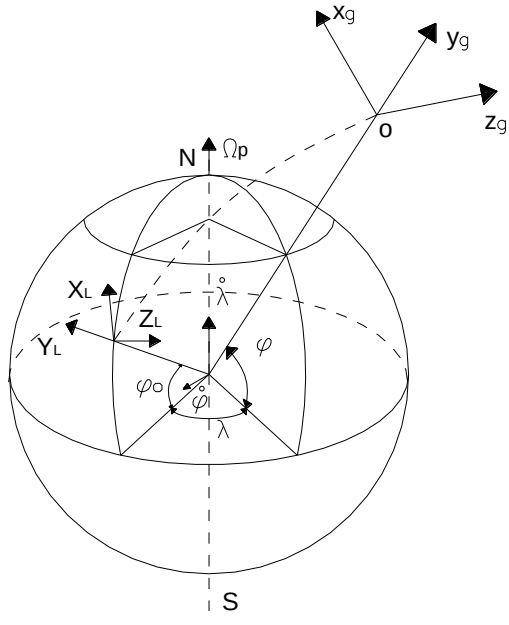

Figure 2. The Geocentric and Geographical Frames

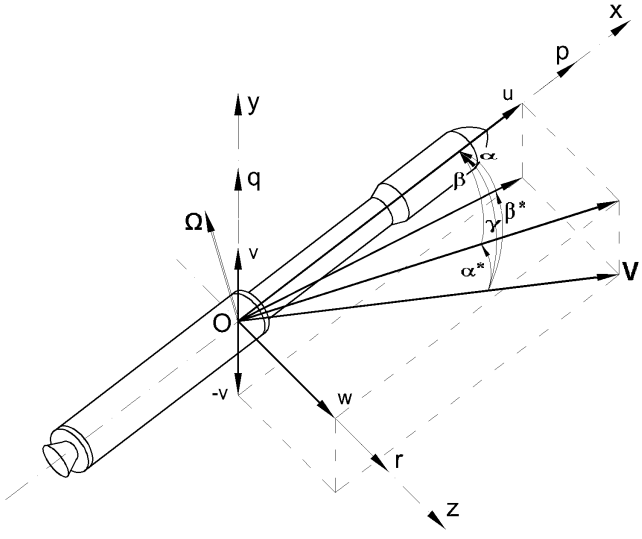

Figure 3. The Body Frame, Velocity Components, Aerodynamic Angles

The Body Frame $Oxyz$

This coordinate system has the origin in the center of launcher mass (Figure 3). The axis x is located along the longitudinal symmetry axis of the body. Axis y is located in the symmetry plane of the vehicle. The deriving Z axis, forms a right trihedral with first two axes. Afterwards, we use this trihedral to write dynamic equations of rotation around the mass center.

Also it will be use to write thrust terms and also aerodynamic terms.

The Velocity Frame $Ox_a y_a z_a$

This coordinate system has the origin in center of the launcher mass. The axis x_a of this trihedral is placed along the velocity vector $\mathbf{V}$. The axis y_a and z_a are in a perpendicular plane of the velocity vector, which in turn is tangent to the trajectory. Axis y_a is located in the symmetry plane of the vehicle. The deriving z axis forms a right trihedral with the first two axes. Next we use this trihedral to write aerodynamic terms, thus it is also called aerodynamic trihedral.

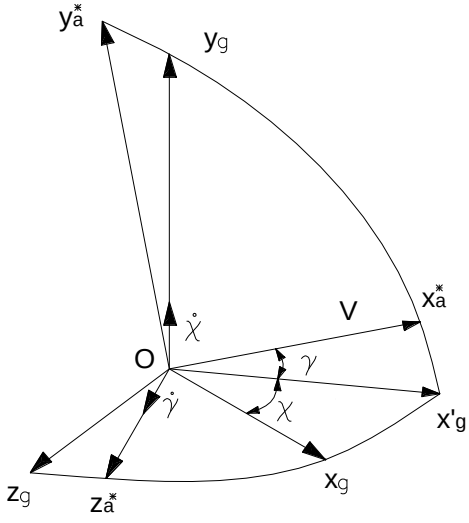

Figure 4. The rotations between the geographical frame and quasi-velocity frame

The Quasi-Velocity Frame $Ox_a^*y_a^*z_a^*$

This coordinate system has the origin in center of the launcher mass (Figure 4). Similarly to velocity frame, the quasi-velocity frame has the axis x_a^* located along the velocity vector, but the axis y_a^* it is in vertical plane. The deriving z_a^* axis, forms a right trihedral with the first two axes. Next we will use the trihedral to write dynamic translation motion equations of the mass center.

3. COORDINATE TRANSFORMATIONS

The rotation matrix between the body frame $Oxyz$ and the aerodynamic frame $Ox_a, y_a z_a$ used for aerodynamics terms is presented in paper [2], [4], [5], [6]. The rotation matrix between the body frame $Oxyz$ and the quasi-velocity frame $Ox_a^*y_a^*z_a^*$ is:

$$\mathbf{A}_{\alpha\beta^*\mu} = \begin{bmatrix} \cos\alpha\cos\beta^* & \sin\alpha\cos\mu + \cos\alpha\sin\beta^*\sin\mu & \sin\alpha\sin\mu - \cos\alpha\sin\beta^*\cos\mu \\ -\sin\alpha\cos\beta^* & \cos\alpha\cos\mu - \sin\alpha\sin\beta^*\sin\mu & \cos\alpha\sin\mu + \sin\alpha\sin\beta^*\cos\mu \\ \sin\beta^* & -\cos\beta^*\sin\mu & \cos\beta^*\cos\mu \end{bmatrix} \tag{1}$$

With this matrix one can express different values from the quasi- velocity frame in body frame. If it is necessary to express values from the body frame in quasi-velocity frame, like thrust components, we can use the inverse of this matrix, which is identical with the transpose of the matrix $A_{\alpha\beta^*\mu}$. Using Figure 4 we obtain the rotation matrix between the geographical frame and quasi-velocity frame:

$$\mathbf{A}_{\gamma\chi} = \begin{bmatrix} \cos\gamma & \sin\gamma & 0 \\ -\sin\gamma & \cos\gamma & 0 \\ 0 & 0 & 1 \end{bmatrix} \begin{bmatrix} \cos\chi & 0 & -\sin\chi \\ 0 & 1 & 0 \\ \sin\chi & 0 & \cos\chi \end{bmatrix} = \begin{bmatrix} \cos\chi\cos\gamma & \sin\gamma & -\sin\chi\cos\gamma \\ -\cos\chi\sin\gamma & \cos\gamma & \sin\chi\sin\gamma \\ \sin\chi & 0 & \cos\chi \end{bmatrix} \tag{2}$$

In this case, we can write the link between the body frame and the geographical frame:

$$\begin{bmatrix} x & y & z \end{bmatrix}^T = \mathbf{A}_{\alpha\beta^*\mu}\mathbf{A}_{\gamma\chi}\begin{bmatrix} x_g & y_g & z_g \end{bmatrix}^T = \mathbf{A}_{\alpha\beta^*\mu\gamma\chi}\begin{bmatrix} x_g & y_g & z_g \end{bmatrix}^T \tag{3}$$

4. THE EQUATIONS OF MOTION IN QUASI-VELOCITY FRAME

Because the quasi-velocity frame is not an inertial frame, the dynamic equation of motion in quasi-velocity frame has the following form:

$$\frac{\partial \mathbf{V}}{\partial t} + \mathbf{\Omega}_V^* \times \mathbf{V} = \frac{\mathbf{N}}{m} + \mathbf{g} + \mathbf{a}_c \,, \tag{4}$$

where we have grouped the aerodynamic and thrust forces.

$$\mathbf{N} = \mathbf{F} + \mathbf{T} \tag{5}$$

And Coriolis acceleration is:

$$\mathbf{a}_c = -2\mathbf{\Omega}_p \times \mathbf{V} \tag{6}$$

The locale derivative of the velocity in quasi-velocity frame is $\partial \mathbf{V}/\partial t$, and $\mathbf{\Omega}_V^*$ is the rotation velocity of the quasi-velocity frame related the local frame, which can be expressed in vectorial form:

$$\mathbf{\Omega}_V^* = \dot{\boldsymbol{\gamma}} + \dot{\boldsymbol{\chi}} + \dot{\boldsymbol{\varphi}} + \dot{\boldsymbol{\lambda}} \tag{7}$$

The derivatives of latitude and longitude angles along the geographical frame are:

$$\dot{\boldsymbol{\lambda}} = \dot{\lambda}\left(\mathbf{i}_g \cos\varphi + \mathbf{j}_g \sin\varphi\right); \; \dot{\boldsymbol{\varphi}} = -\mathbf{k}_g \dot{\varphi} \tag{8}$$

where $\mathbf{i_g}, \mathbf{j_g}, \mathbf{k_g}$ are unitary vectors in geographical frame.

If we make the projection along the quasi-velocity frame it results:

$$\begin{gathered} \dot{\boldsymbol{\lambda}} = \dot{\lambda}\left[\mathbf{i}_a\left(\cos\varphi\cos\chi\cos\gamma + \sin\varphi\sin\gamma\right) + \mathbf{j}_a\left(-\cos\varphi\cos\chi\sin\gamma + \sin\varphi\cos\gamma\right) + \mathbf{k}_a\left(\cos\varphi\sin\chi\right)\right] \\ \dot{\boldsymbol{\varphi}} = \dot{\varphi}\left[\mathbf{i}_a \sin\chi\cos\gamma - \mathbf{j}_a \sin\chi\sin\gamma - \mathbf{k}_a \cos\chi\right] \end{gathered} \tag{9}$$

The derivatives of the climb angle and air - path track angle are:

$$\dot{\boldsymbol{\chi}} = \dot{\chi}\left(\mathbf{i}_a \sin\gamma + \mathbf{j}_a \cos\gamma\right) \;\; \dot{\boldsymbol{\gamma}} = \dot{\gamma}\mathbf{k}_a \tag{10}$$

In this case, the components of angular velocity vector along quasi-velocity frame become:

$$\begin{aligned} \omega_l^* &= \dot{\lambda}\left(\cos\varphi\cos\chi\cos\gamma + \sin\varphi\sin\gamma\right) + \dot{\varphi}\sin\chi\cos\gamma + \dot{\chi}\sin\gamma \\ \omega_m^* &= \dot{\lambda}\left(-\cos\varphi\cos\chi\sin\gamma + \sin\varphi\cos\gamma\right) - \dot{\varphi}\sin\chi\sin\gamma + \dot{\chi}\cos\gamma \\ \omega_n^* &= \dot{\lambda}\cos\varphi\sin\chi - \dot{\varphi}\cos\chi + \dot{\gamma} \end{aligned} \tag{11}$$

Taking in consideration that the vector $\mathbf{\Omega}_p$ has the same orientation with vector $\dot{\boldsymbol{\lambda}}$, we can write:

$$\mathbf{\Omega}_p = \Omega_p \begin{bmatrix} \mathbf{i}_a\left(\cos\varphi\cos\chi\cos\gamma + \sin\varphi\sin\gamma\right) + \mathbf{j}_a\left(\sin\varphi\cos\gamma - \cos\varphi\cos\chi\sin\gamma\right) + \\ \mathbf{k}_a\left(\cos\varphi\sin\chi\right) \end{bmatrix}, \tag{12}$$

for where Coriolis acceleration components in quasi-velocity frame are:

$$\begin{gathered} a_{cx} = 0\,; \; a_{cy} = -2V\Omega_{pz} = -2V\Omega_p \cos\varphi\sin\chi\,; \\ a_{cz} = 2V\Omega_{py} = 2V\Omega_p\left(\sin\varphi\cos\gamma - \cos\varphi\cos\chi\sin\gamma\right) \end{gathered} \tag{13}$$

The gravitational acceleration is presented in detail in papers [2], [6], being finally expressed by two terms, one term denoted g_r oriented along the radius r and the other term g_ω parallel with polar axis $N-S$. These two terms contain gravitational components and also centrifugal components given by Earth spin.

$$g_r = g_{Ar} - \Omega_p^2 r\,; \qquad g_\omega = g_{A\omega} + \Omega_p^2 r \sin\varphi\,, \tag{14}$$

where g_{Ar} and $g_{A\omega}$ are given by work [6], [8], being obtained by so-called „J_2“model, that allows to take into account the influence of the flattened shape of the Earth, depending of the latitude angle φ:

$$g_{Ar} = \frac{a_{00}}{r^2} - \frac{3}{2}\frac{a_{20}}{r^4}(5\sin^2\varphi - 1) + \ldots; \quad g_{A\omega} = 3\frac{a_{20}}{r^4}\sin\varphi - \ldots\cdot \tag{15}$$

Next we will project the terms given by relation (14) along the quasi-velocity frame. For this keep in mind that term g_r is along the angular velocity vector $\dot{\chi}$ given by relation (9) and term g_ω is along the angular velocity vector $\dot{\lambda}$ given by relation (9) opposite to it. In this case we have:

$$\begin{aligned} g_x &= -g_r\sin\gamma - g_\omega(\cos\varphi\cos\chi\cos\gamma + \sin\varphi\sin\gamma);\\ g_y &= -g_r\cos\gamma - g_\omega(-\cos\varphi\cos\chi\sin\gamma + \sin\varphi\cos\gamma);\ g_z = -g_\omega\cos\varphi\sin\chi\,. \end{aligned} \tag{16}$$

Summarizing, starting from relation (4), we obtain the dynamic equation which describes the motion of the launcher mass in quasi-velocity frame:

$$\begin{aligned} \dot{V} &= \frac{D}{m} + \frac{X^T}{m}\cos\alpha\cos\beta^* - \frac{Y^T}{m}\sin\alpha\cos\beta^* + \frac{Z^T}{m}\sin\beta^* -\\ &\quad - g_r\sin\gamma - g_\omega(\cos\varphi\cos\chi\cos\gamma + \sin\varphi\sin\gamma)\\ \dot{\gamma} &= \frac{L}{mV}\cos\mu - \frac{N}{mV}\sin\mu + \frac{X^T}{mV}(\sin\alpha\cos\mu + \cos\alpha\sin\beta^*\sin\mu) +\\ &\quad + \frac{Y^T}{mV}(\cos\alpha\cos\mu - \sin\alpha\sin\beta^*\sin\mu) - \frac{Z^T}{mV}\cos\beta^*\sin\mu -\\ &\quad - \frac{g_r}{V}\cos\gamma - \frac{g_\omega}{V}(-\cos\varphi\cos\chi\sin\gamma + \sin\varphi\cos\gamma) + \frac{V}{r}\cos\gamma - 2\Omega_p\cos\varphi\sin\chi\\ \dot{\chi} &= -\frac{L}{mV}\frac{\sin\mu}{\cos\gamma} - \frac{N}{mV}\frac{\cos\mu}{\cos\gamma} - \frac{X^T}{mV}\frac{(\sin\alpha\sin\mu - \cos\alpha\sin\beta^*\cos\mu)}{\cos\gamma} -\\ &\quad - \frac{Y^T}{mV}\frac{(\cos\alpha\sin\mu + \sin\alpha\sin\beta^*\cos\mu)}{\cos\gamma} - \frac{Z^T}{mV}\frac{\cos\beta^*\cos\mu}{\cos\gamma} +\\ &\quad + \frac{g_\omega\cos\varphi\sin\chi}{V\cos\gamma} + \frac{V}{r}\tan\varphi\sin\chi\cos\gamma + 2\Omega_p(\cos\varphi\cos\chi\tan\gamma - \sin\varphi) \end{aligned} \tag{17}$$

complemented with kinematic equations:

$$\dot{\varphi} = \frac{V}{r}\cos\chi\cos\gamma\ ; \dot{\lambda} = -\frac{V\sin\chi\cos\gamma}{r\cos\varphi}; \dot{r} = V\sin\gamma\,. \tag{18}$$

Regarding the dynamic equations of the rotational motion around the center of mass, written in body frame, and resuming the results obtained in paper [2] we obtain:

$$\dot{p} = \frac{L^T + L^A}{A} + \frac{B-C}{A} qr\,;\ \dot{q} = \frac{M^T + M^A}{B} + \frac{C-A}{B} rp\,;\ \dot{r} = \frac{N^T + N^A}{C} + \frac{A-B}{C} pq \quad (19)$$

From the previous relations we can observe that for obtaining the components of the aerodynamic force and the detraction force in the quasi-velocity frame we need the angles connecting the quasi-velocity frame from the body frame.

These angles are: α, β^* and μ. In order to obtain them in the form of differential equations we must take into account that if the angular velocity in the body frame is $\Omega = \begin{bmatrix} p & q & r \end{bmatrix}^T$ in reference to an inertial frame and the angular speed of the quasi-velocity frame referenced to a local frame is $\mathbf{\Omega}_V^* = \begin{bmatrix} \omega_l^* & \omega_m^* & \omega_n^* \end{bmatrix}^T$, between the two vectors the following equation is true:

$$\mathbf{\Omega} = \mathbf{\Omega}_V^* + \dot{\boldsymbol{\mu}} + \dot{\boldsymbol{\beta}}^* + \dot{\boldsymbol{\alpha}} + \mathbf{\Omega}_p \quad (20)$$

If we project this equation on the axes of the body frame we obtain:

$$\begin{bmatrix} p \\ q \\ r \end{bmatrix} = A_{\alpha\beta^*\mu} \begin{bmatrix} 0 \\ \omega_m^* \\ \omega_n^* \end{bmatrix} + A_{\alpha\beta^*} \begin{bmatrix} \omega_l^* + \dot{\mu} \\ \dot{\beta}^* \\ 0 \end{bmatrix} + \begin{bmatrix} 0 \\ 0 \\ \dot{\alpha} \end{bmatrix} + \Omega_p A_I \begin{bmatrix} \cos\varphi_0 \cos\psi_0 \\ \sin\varphi_0 \\ -\cos\varphi_0 \sin\psi_0 \end{bmatrix} \quad (21)$$

by substituting the matrixes:

$$\begin{bmatrix} p \\ q \\ r - \dot{\alpha} \end{bmatrix} = \begin{bmatrix} \cos\alpha\cos\beta^* & \sin\alpha\cos\mu + \cos\alpha\sin\beta^*\sin\mu & \sin\alpha\sin\mu - \cos\alpha\sin\beta^*\cos\mu \\ -\sin\alpha\cos\beta^* & \cos\alpha\cos\mu - \sin\alpha\sin\beta^*\sin\mu & \cos\alpha\sin\mu + \sin\alpha\sin\beta^*\cos\mu \\ \sin\beta^* & -\cos\beta^*\sin\mu & \cos\beta^*\cos\mu \end{bmatrix}$$
$$\begin{bmatrix} 0 \\ \omega_m^* \\ \omega_n^* \end{bmatrix} + + \begin{bmatrix} \cos\alpha\cos\beta^* & \sin\alpha & -\cos\alpha\sin\beta^* \\ -\sin\alpha\cos\beta^* & \cos\alpha & \sin\alpha\sin\beta^* \\ \sin\beta^* & 0 & \cos\beta^* \end{bmatrix} \begin{bmatrix} \omega_l^* + \dot{\mu} \\ \dot{\beta}^* \\ 0 \end{bmatrix} + \begin{bmatrix} \Omega_{pp} \\ \Omega_{pq} \\ \Omega_{pr} \end{bmatrix} \quad (22)$$

From where we get the following scalar connections;

$$\begin{aligned} p^* &= (\omega_l^* + \dot{\mu})\cos\alpha\cos\beta^* + \dot{\beta}^*\sin\alpha + \omega_m^* a_{12} + \omega_n^* a_{13} \\ q^* &= -(\omega_l^* + \dot{\mu})\sin\alpha\cos\beta^* + \dot{\beta}^*\cos\alpha + \omega_n^* a_{22} + \omega_n^* a_{23} \\ r^* &= (\omega_l^* + \dot{\mu})\sin\beta^* + \dot{\alpha} + \omega_m^* a_{3,2} + \omega_n^* a_{33} \end{aligned} \quad (23)$$

where we denoted with a_{ij} the elements of the $A_{\alpha\beta^*\mu}$ matrix and the rotation velocities after the axes connected to the body:

$$p^* = p - \Omega_{pp};\ q^* = q - \Omega_{pq};\ r^* = r - \Omega_{pr} \quad (24)$$

If we continue the calculation:

$$\begin{aligned}(\omega_l^* + \dot{\mu})\cos\alpha\cos\beta^* + \dot{\beta}^*\sin\alpha &= p^* - \omega_m^* a_{12} - \omega_n^* a_{13}\\ -(\omega_l^* + \dot{\mu})\sin\alpha\cos\beta^* + \dot{\beta}^*\cos\alpha &= q^* - \omega_n^* a_{22} - \omega_n^* a_{23}\\ (\omega_l^* + \dot{\mu})\sin\beta^* + \dot{\alpha} &= r^* - \omega_m^* a_{3,2} - \omega_n^* a_{33}\end{aligned} \tag{25}$$

and we finally get:

$$\begin{aligned}\dot{\mu} &= p^*\frac{\cos\alpha}{\cos\beta^*} - q^*\frac{\sin\alpha}{\cos\beta^*} - \omega_l^* - \left(\omega_m^*\sin\mu - \omega_n^*\cos\mu\right)\tan\beta^*\\ \dot{\beta}^* &= p^*\sin\alpha + q^*\cos\alpha - \omega_m^*\cos\mu - \omega_n^*\sin\mu\\ \dot{\alpha} &= -p^*\cos\alpha\tan\beta^* + q^*\sin\alpha\tan\beta^* + r^* + \omega_m^*\frac{\sin\mu}{\cos\beta^*} - \omega_n^*\frac{\cos\mu}{\cos\beta^*}\end{aligned} \tag{26}$$

Where the angular velocity components in the body frame p, q, r can be found from the dynamic equations written around the center of mass (19) and the components of the angular velocity of the quasi-velocity frame $\omega_l^*, \omega_m^*, \omega_n^*$ are given by equation (11).

The systems of equations (17), (18), (19) and (26) represent the movement equations of the unguided rocket. In order to construct the guided movement equations we must add the guidance equations or the guidance commands.

5. NONLINEAR RELATIONS FOR GUIDANCE AND CONTROL

Resuming paper [2], [3] the guidance command for SOL is described by following relation:

$$\mathbf{u} = \mathbf{u}_b - \mathbf{T}_{u1}\left[u_\phi \;\; u_\psi \;\; u_\theta\right]^T - \mathbf{T}_{u2}\left[0 \;\; 0 \;\; u_z\right]^T - \mathbf{T}_{u3}\left[0 \;\; u_\beta + u_{\delta_m} \;\; u_\alpha + u_{\delta n}\right]^T \tag{27}$$

where the command signals have the significance u_z - Lateral linear deviation signal; u_ϕ - Roll signal; u_θ - Pitch signal; u_ψ - Yaw signal; u_α - incidence signal; u_β -Sideslip signal; $u_{\delta n}$ - Yaw angular deflection signal; $u_{\delta m}$ - Pitch angular deflection signal.

Summarizing the above relations, we can write the guidance command (27) in scalar form:

$$\begin{aligned}u_l &= -u_\phi + u_\theta\sin\psi;\\ u_m &= -u_\psi\cos\phi - u_\theta\sin\phi\cos\psi + u_z\cos\phi\cos\psi - u_\beta - u_{\delta m};\\ u_n &= u_{nb} + u_\psi\sin\phi - u_\theta\cos\phi\cos\psi - u_z\sin\phi\cos\psi - u_\alpha - u_{\delta n};\end{aligned} \tag{28}$$

6. CALCULUS ALGORITHM, INPUT DATA, TEST CASE

Algorithm

The calculus algorithm consists in multi-step method Adams' predictor-corrector with variable step integration method [1], [9], [10]. Absolute numerical error was 1.e-12, and relative error was 1.e-10.

Input Data for SOL Model

The mechanical characteristics for SOL are included in Table 1.

Table 1 Mechanical Characteristics

Configuration	Mass m [T]		Center of mass (from the bottom) x_{cm} [m]		Axial Moment of Inertia A [Tm^2]		Transverse Moment of Inertia B [Tm^2]	
	Initial	Final	Initial	Final	Initial	Final	Initial	Final
Stage I + II + III + AVUM + P/L	34.7	10.7	10.3	6.1	17.8	3.9	550.1	129.7
Stage II + III + AVUM + P/L	8.5	2.6	4.7	2.8	2.0	0.7	31.7	6.1
Stage III + AVUM + P/L	2.0	0.6	2.2	1.5	0.5	0.2	1.1	0.4
AVUM + P/L	0.49	0.38	1.3	1.2	0.15	0.11	0.17	0.13
P/L	0.1	0.1	0.25	0.25	0.01	0.01	0.01	0.01

For determining the launcher aerodynamics properties, we used a methodology based on paper [7]. Thrust characteristics for SOL3 are presented in table 2.

Table 2 Thrust Characteristics - V - Vaccum

Stage	Specific impulse I_{sp} [s]	Propellant mass m_p [T]	Total Impulse I_Σ [kNs]	Duration t [s]
I (V)	280	23.9	65649	72
II (V)	290	5.9	16785	45
III (V)	295	1.4	4051	45
AVUM (V)	315	0.11	340	200

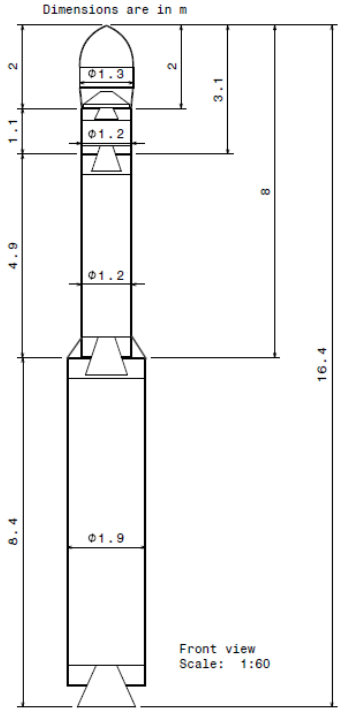

Figure 5. SOL geometry

Test case:

As test case, the following initial conditions were used: Geographic orientation: Azimuth angle $\psi_0 = 115°$ (towards the South - East); Geocentric latitude $\varphi_0 = 45°$ (Romania latitude); Altitude: $y_0 = 1[m]$; Initial velocity $V_0 = 1[m/s]$; Initial climb angle $\gamma_0 = 90°$. In order to evaluate the risk zone, we consider the following worst scenarios:

During the ascensional phase, the guidance system applies a lateral commands corresponding to different yaw angles. After first stage or after second stage the launcher motor stops and the launcher or parts of it follows a ballistic unguided trajectory.

The risk zone is given by the horizontal projection of all possible trajectories. Actually, the two risk zones obtained correspond with the area where the first stage or the second stage of the launcher is possible to fall.

7. RESULTS

Evaluation risk zone for the first stage

As we have previously mentioned, for obtaining the maximum dispersal of trajectories in horizontal plane, we assumed the occurrence of a navigation error which generates a lateral guidance signal which is linear, as shown in Figure 6, which then takes the form of 7 distinct angular values. As a result of these wrong commands, during the functioning of the first step we get attitude errors, as shown in Figure 7.

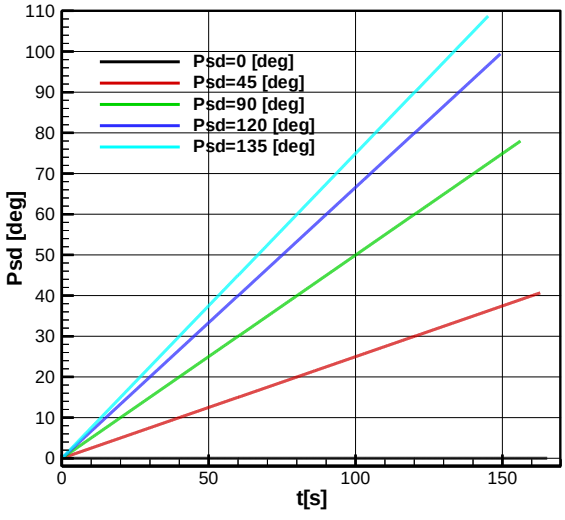

Figure 6. Imposed commands for lateral maneuver SOL 2

We can observe from this figure that after the first step stops functioning, the head angle value remains constant, case which corresponds to a ballistic evolution that can be achieved only by the first step of the launcher after the detachment or by the entire launcher if the second step does not fire, or by the center of mass of the elements resulting in the case of an explosion at the end of the first step's functioning. Following the 7 error cases analyzed in Figure 8 we present a beam of velocities and in Figure 9 we present the diagram of the 7 possible trajectories in vertical plane. Finally, after we make a horizontal projection of 7 possible trajectories, we obtain the risk semi-zone for the first step, which is presented in Figure 10.

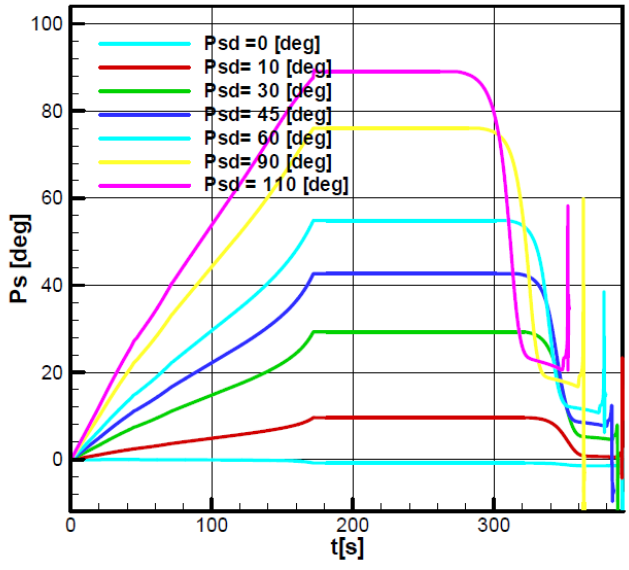

Figure 7. Achieved commands for lateral maneuver SOL2

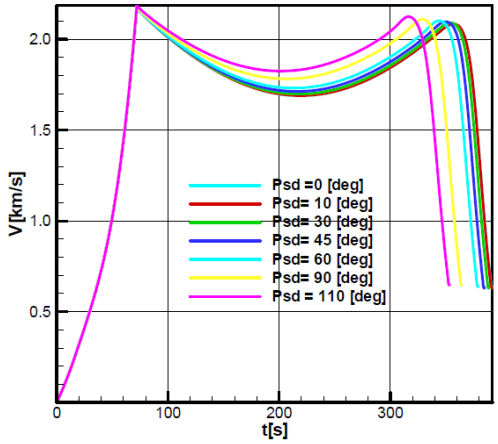

Figure 8. Velocity diagram SOL

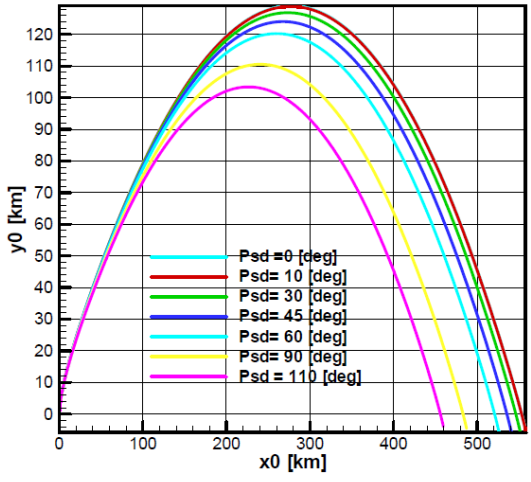

Figure 9. Trajectory diagram – vertical plane SOL

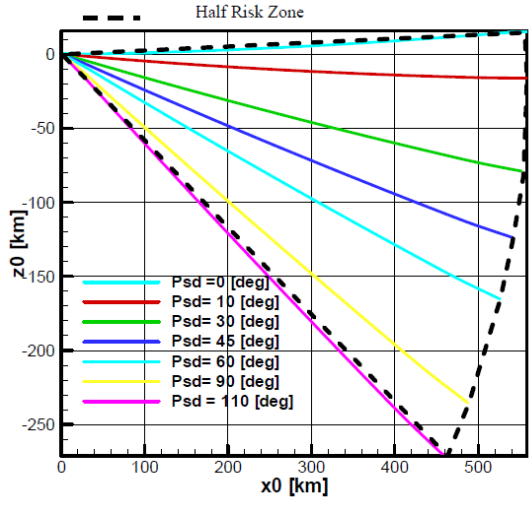

Figure 10. Trajectory diagram – horizontal plane. Risk zone first stage SOL

Evaluation risk zone for second stage

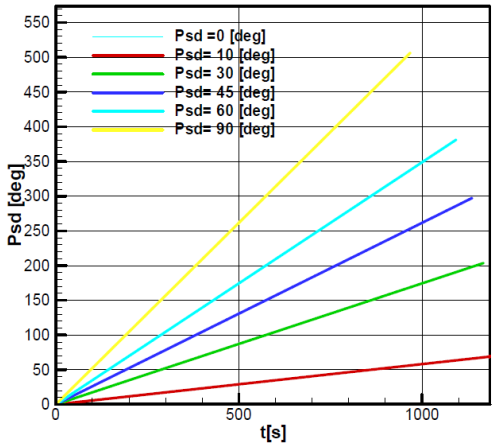

Figure 11. Imposed commands for lateral maneuver - SOL

We act similarly in the case of the second stage. Therefore, in Figure 11 we present a beam of 6 erroneous lateral maneuvers which may occur during the functioning of the first two stages. In Figure 12 we present the head angles that may occur because of the navigation errors. In Figure 13 we present the velocity diagrams corresponding to the functioning of the two stages. In Figure 14 we present the trajectories beam in the vertical plane and in Figure 15 we present the trajectories beam in the horizontal plane, which represents the risk semi-zone for the second stage of the launcher.

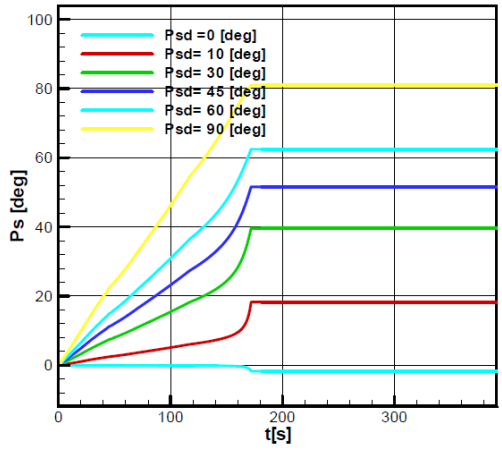

Figure 12. Achieved commands for lateral maneuver – SOL2

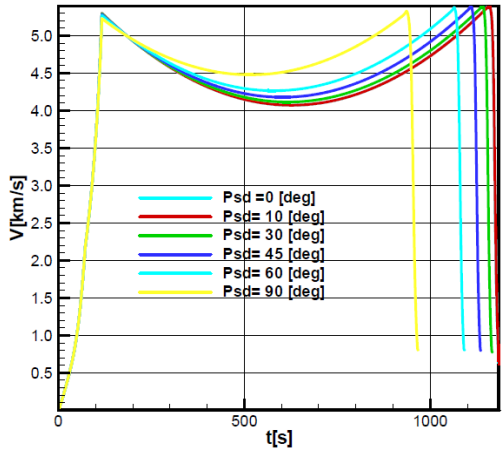

Figure 13. Velocity diagram – SOL2

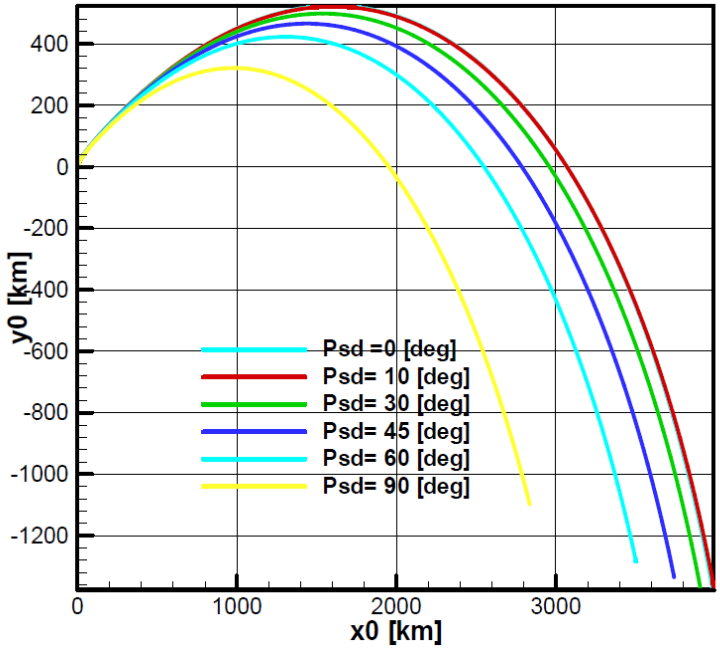

Figure 14. Trajectory diagram – vertical plane – SOL2

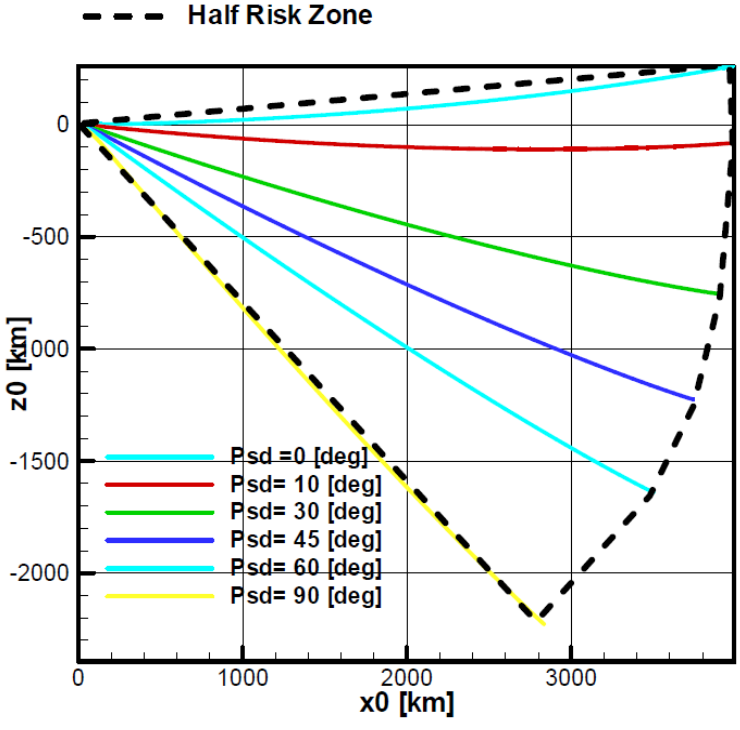

Figure 15. Trajectory diagram –horizontal plane. Risk zone second stage SOL

In Figure 16 are presented risk area for the first stage and in Figure 17 for the second stage in case of launching from Romania (Capu Midia fairing range) in inclined orbit $i = 54°$.

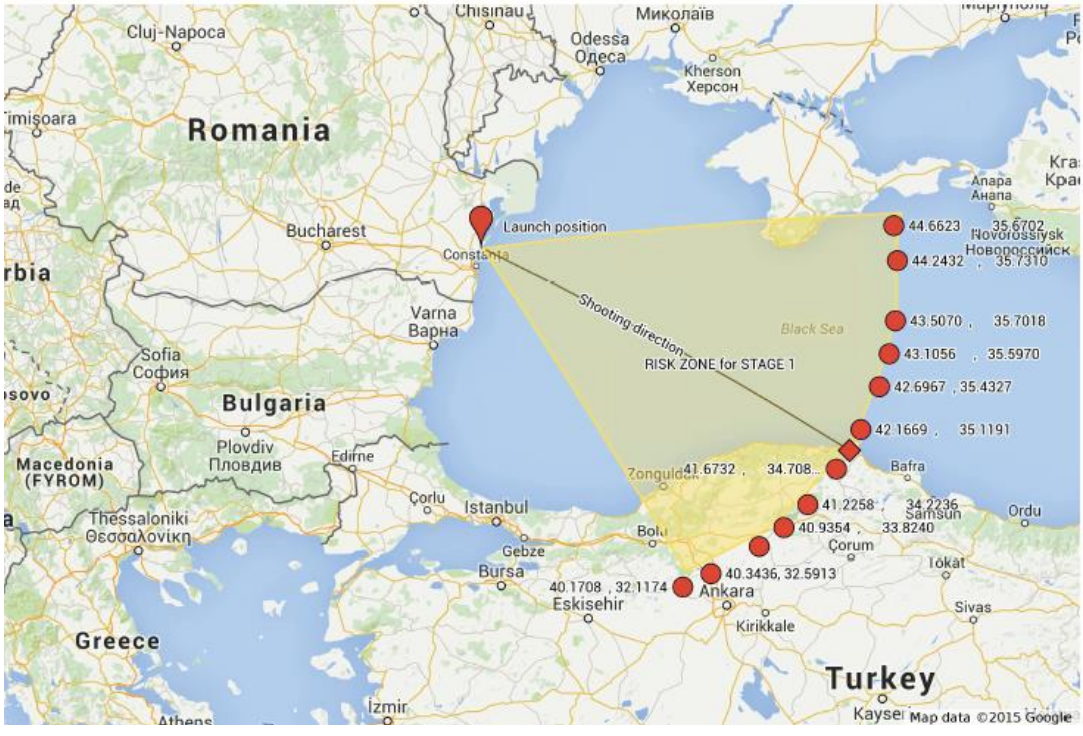

Figure16. Risk Zone for SOL stage 1 in Romania launch case

Figure17. Risk Zone for SOL stage 2 in Romania launch case

7. CONCLUSIONS

We developed two mathematical models to evaluate the risk zone. The first one was built in the start frame and was used for the ascensional guided phase because the guidance relations is more convenient to be written in this frame. In second phase of the evolution when the rotational motion is more difficult to be described due to dynamic instability, we have built the second mathematical model based on *quasi – velocity frame* that contains only translational equations, enough for describe this ballistic motion of the launcher or its parts. Using these two models and considering the worst scenarios we have obtained the horizontal dispersal of the trajectories defining the risk zone. Risk zones were evaluated in two situations: after the separation of the first stage and after the separation of the second stage of the launcher. These two zones also represent the possible area where the first or the second stage of the launcher will fall. The results obtained can be used to choose the launching location for SOL. As we can see in Figure 16 and Figure 17, from the risk zones point of view, launching from Romania is not convenient because the risk zones overlap populated areas of the states in the vicinity of the base trajectory, which is not allowable from a firing safety point of view.

ACKNOWLEDGEMENT

The work has been funded by the Sectoral Operational Programme Human Resources Development 2007 - 2013 of the Ministry of European Funds thought the Financial Agreement POSDRU/159/1.5/S/132395.

REFERENCES

[1] N. Bakhvalov, *Méthodes Numériques – Analyse, algèbre, équations différentielles ordinaires*, Ed. Mir Moscou, 1976.

[2] T. V. Chelaru, *Dinamica Zborului – Racheta dirijată, Ed a-II-a revizuita şi adaugită*, (*Dynamnic Flight – The Guided Missile- 2nd Eddition Enlarged*), Ed.Printech, ISBN 973-718-013-5, Bucureşti, 434 pag., mai 2004.

[3] T. V. Chelaru, A. Chelaru, *Mathematical Model and Performance Evaluation for a Small Orbital Launcher*, Proceedings of International Conference on Advanced research in Aerospace, Robotics, Manufacturing Systems, Mechanical Engineering and Bioengineering (OPTIROB 2015), ISBN -13: 978-5-03835-502-1, Applied Mechanics and Materials, Vol **772**, pp. 388-394, www.scientific.net, Jupiter, Constanta, Romania, June 26-29, 2015.

[4] T. Hacker, *Stabilitate şi comandă în teoria zborului,* Ed. Academiei, Bucureşti, 1968.

[5] Н. Т. Кузовков, *Системы стабилизации летателных аппаратов, балистических и зенитных ракет,* Издателъство «Высшая школа», Москва, 1976.

[6] А. А. Лебедев, Н. Ф. Герасюта, *Балистика ракет,* Издателъство «Машиностроение», Москва, 1970.

[7] J. N. Nielsen, *Missile Aerodynamics*, McGraw-Hill Book Company, Inc., New-York, Toronto, London, 1960.

[8] M. M. Niţă, D. Şt. Andreescu, *Zborul rachetei*, Ed. Militară, Bucureşti, 1964.

[9] * * * *SLATEC 3.0 (Mthematical General Linrary) Bibliotecă matematică generală de programe în limbaj FORTRAN*, realizată de următoarele laboratoare de cercetări: Air Force Weapons Laboratory; Lawrence Livermore National Laboratory; Los Alamos National Laboratory; Magnetic Fusion Energy Computing Center; National Bureau of Standards; Sandia National Laboratories (Albuquerque & Livermore); Martin Marietta Energy Systems; Incorporated at Oak Ridge National Laboratory, SUA, 1986.

[10] * * * SANDIA – (dedicated FORTRAN Library), elaborata de: LFC – Laboratorul de Fizica Computationala – Univ. Iasi, ADZ –Laboratorul de Aerodinamică şi Dinamica Zborului din cadrul UM 02481- Ploieşti, UPB-CCAS – Centrul de Cercetări pentru Aeronautică şi Spaţiu din cadrul UPB – Bucureşti.